IOP PUBLISHING JOURNAL OF PHYSICS: CONDENSED MATTER

J. Phys.: Condens. Matter **19** (2007) 305004 (13pp) doi:10.1088/0953-8984/19/30/305004

TOPICAL REVIEW

Structure and dynamics of Xe monolayers adsorbed on Cu(111) and Pt(111) surfaces studied in the density functional approach

P Lazić[1], R Brako[1] and B Gumhalter[2]

[1] Rudjer Bošković Institute, 10000 Zagreb, Croatia
[2] Institute of Physics, 10000 Zagreb, Croatia

Received 5 February 2007, in final form 7 March 2007
Published 13 July 2007
Online at stacks.iop.org/JPhysCM/19/305004

Abstract

We review theoretical treatments of physisorption of Xe on Cu(111) and Pt(111) surfaces within the recently proposed extended density functional approach that explicitly takes into account the van der Waals interactions among the constituents of adsorption systems. Based on tests of the various currently used approximations for the density functionals, and of the different treatments of long-range correlation effects which we carried out for a prototype system of a Kr dimer, we have adopted in the present study the schemes that are appropriate to systems consisting of nearly isolated fragments. In this approach the coefficients of van der Waals expansion are deduced from the DFT calculations of intrafragment electronic densities. Such generalized DFT calculations of potential energy surfaces yield a structure of Xe adlayers in good agreement with experiments and retrieve the dilation of the commensurate monolayer phase with strongly reduced intralayer Xe–Xe radial force constants. This approach provides a *first principles* interpretation of the observed vibrational properties of commensurate adlayers of Xe physisorbed on Cu(111) and Pt(111) surfaces.

(Some figures in this article are in colour only in the electronic version)

Contents

0953-8984/07/305004+13$30.00

1. Introduction

For decades rare gas overlayers have served as benchmark systems for studying the interaction potentials that govern physical adsorption on solid surfaces. A proper theoretical description of this class of systems is a long-standing challenge of great importance for the interpretation of adsorption and related phenomena [1]. A popular qualitative picture of the potentials causing physisorption of rare gas atoms has been that of a sum of the long-range attractive van der Waals (vdW) and the short range Pauli repulsion components acting between the electronic charge densities of the substrate and the adatoms [2]. In many circumstances a representation of the total adatom–substrate interaction by the sum of empirical binary potentials has given reasonable results for adsorption energies [3]. According to this recipe the highly coordinated lattice sites naturally arise as preferred adsorption sites for the adatoms. However, recent experiments on the commensurate $(\sqrt{3} \times \sqrt{3})$R30° Xe monolayers adsorbed on Cu(111) [4] and Pt(111) [5] surfaces have contradicted this simple picture in two important aspects: (i) the adsorption sites for Xe atoms deduced from the measurements were on top of the Cu [6] and Pt [7, 8] atoms instead in the highly coordinated threefold hollow sites, and (ii) the frequencies of in-plane vibrations in monolayer Xe/Cu(111) as measured by He atom scattering (HAS) [9–11] turned out lower than could have been expected from the force constants calculated for *unconstrained* Xe adlayers by using accurate pairwise atomic gas phase potentials [12]. Similar observations were also made for Xe adsorption on Cu(100) [10] and Cu(110) [13] surfaces. For Xe/Pt(111) the absence of any significant dispersion of in-plane vibrations in the dilated commensurate Xe monolayer prevented unambiguous assignments of the measured dispersion curves [14]. Attempts to provide a unified interpretation of these findings within the various empirical approaches to physisorption [1–3] were unsuccessful, and resort to an analysis based on *ab initio* approaches proved indispensable.

The first *ab initio* studies of Ar and Xe adsorption on metals employing the density functional theory in the local density approximation [15] (DFT-LDA) were carried out for a jellium surface [16]. However, for adsorption on real metals a more realistic atomistic representation of the substrate was required. This was undertaken in cluster calculations of adsorption of one and two Xe atoms on a Pt(111) surface within the DFT-LDA [17], which showed the preferred on-top adsorption sites, and more recently for adsorption of Xe on top of Cu(111) in the wave function self-consistent field approach, with the inclusion of vdW attraction as a correlation effect in second order perturbation theory [18]. However, despite the reasonable results obtained for adsorption energy [17] and perpendicular vibration frequency [18], these calculations proved to be of limited use. Primarily this was due to the neglect of the periodic atomic and ensuing electronic band structure of the underlying substrate and thereby of the experimentally detected broadening of adsorbate valence and affinity levels [19, 20], namely the occupied 5p and unoccupied 6s and 6p Xe atomic orbitals. This deficiency of the cluster approach was removed in later LCAO calculations of adsorption of isolated Xe atoms on an Al(100) surface [21]. The total energy calculation in this approach combined the contributions from short-range adatom–surface interactions obtained from the treatment of a many-body Hamiltonian in a tight binding representation, and from adatom–planar surface vdW interactions treated separately by standard methods. These calculations showed explicitly the significant role played by the adsorbate 6s affinity level in the formation of a ‘chemisorptive contribution’ to the adatom–surface bonding anticipated in [19]. The obtained

results showed the preference for fourfold hollow over adsorption sites on top for single atoms by ∼20 meV, but monolayer calculations have not been attempted.

The role of the substrate periodic electronic structure in the formation of monolayers was investigated in detail in a comparative DFT-LDA and DFT-generalized gradient approximation (GGA) study of $(\sqrt{3} \times \sqrt{3})$R30° Xe/Pt(111) in [22]. In both cases the binding was strongest at top sites, with LDA overestimating the experimental adsorption energies and vertical adsorbate vibration frequencies, and GGA giving only a shallow and flat adsorption well at large atom–substrate separations. Analogous trends of the DFT-LDA and DFT-GGA results were retrieved in a later study of monolayer Xe adsorption on Mg(0001), Al(111), Ti(0001), Cu(111), Pt(111) and Pd(111) [23]. In these works the binding energies calculated using LDA agreed better with the experimental values. However, it is known that the use of LDA functional leads to the overestimation of binding in systems with inhomogeneous electron density, primarily due to an incorrect description of the exchange energy. Hence, the obtained rough agreement of the LDA results with experimental adsorption energies for the studied systems must be considered as accidental, i.e. for these systems the LDA should not be considered as producing more reliable results than the GGA before all important contributions to the total interaction have been included.

In the DFT calculations quoted above, the role of intra- and interlayer vdW attraction involving Xe adatoms was not taken into account despite the high Xe dynamic polarizability. Hence, for the assessment of validity of the DFT approach the *dynamical polarization* effects that give rise to vdW potentials must be calculated separately but consistently with the obtained electronic densities. We have recently carried out such a programme in the studies of adsorption of commensurate Xe monolayers on Cu(111) and Pt(111) surfaces and reported the results in [24]. Here we present a more detailed discussion of this approach together with some new results pertaining to the studied systems.

2. Density functionals incorporating vdW interactions

Numerical DFT calculations are based on the use of the Kohn–Sham scheme to re-formulate the many-body electron problem in terms of an independent particle system, and the application of an approximate local (LDA) or semilocal, i.e. with terms depending on the density gradient (various flavours of GGA), density functional. These approaches have proved extremely successful in studies of a wide range of molecular and condensed matter systems. The corresponding functionals do not include the electron correlation beyond the semilocal terms, which usually has minor consequences for strongly bound systems. However, the consequences may become significant for systems with small electronic overlap, including the important cases of soft matter, van der Waals complexes, etc. Several attempts have been made to remedy this deficiency by adding the long-range correlation in the form of either asymptotic or damped vdW attraction to the energies calculated in DFT.

Tractable DFT schemes which include the long-range correlation (and hence the vdW interaction) calculated from the DFT electronic densities have recently been developed in [25–28] and [32–34]. Both these approaches are not fully self-consistent, since they use the electron density obtained using a standard DFT functional (usually GGA PW91 or GGA-PBE) as a starting point for calculating the vdW contribution to the energy, but do not recalculate the effects of the latter on the DFT potential. In other words, they assume that the long-range correlation effects, although contributing significantly to the energy of interaction between various parts of the system, are weak enough so that the associated modification of the Kohn–Sham (KS) orbitals (and hence of the total electron density) can be neglected. Available *a posteriori* checks, and in particular the insensitivity of the electronic density of such weakly

interacting systems upon the flavour of the DFT functional used in the calculation, seem to justify this assumption.

2.1. Interfragment approach to van der Waals interactions

In the approach of [25–28] it is assumed that the system consists of well separated 'fragments', e.g. a substrate and a weakly adsorbed atom, and the calculated electron density is used to find the coefficients of (the asymptotic form of) the van der Waals potential acting between the fragments, which is added to the energy obtained from DFT calculations. Thus the intrafragment exchange and correlation effects are still included through the standard DFT functional, which is known to work quite well for separate subsystems (e.g. a metal surface or an atom). The calculation of interfragment interactions starts with the ansatz for the local, i.e. density dependent, frequency of electronic plasma oscillations:

$$\omega_{\mathrm{p}}^2(\mathbf{r}) = \frac{4\pi e^2 n(\mathbf{r})}{m}, \tag{1}$$

where e and $n(\mathbf{r})$ are, respectively, the electron charge and the KS density obtained by using the initially adopted density functional. This is used to construct the intrafragment dielectric tensor in the local approximation:

$$\epsilon_{\alpha,\beta}(\mathbf{r}, \mathbf{r}', \omega) = \delta_{\alpha,\beta}\delta(\mathbf{r} - \mathbf{r}')\epsilon(\mathbf{r}, \omega) \tag{2}$$

with

$$\epsilon(\mathbf{r}, \omega) = 1 - \kappa(n(\mathbf{r}))\frac{\omega_{\mathrm{p}}^2(\mathbf{r})}{\omega^2}. \tag{3}$$

Here $\kappa(n(\mathbf{r}))$ is a conveniently chosen cut-off function [26, 27], without which the local approximation for dielectric response greatly exaggerates the response in the low-density tails.

The leading term in the asymptotic expansion of the vdW interaction potential between two atoms at separation d is:

$$E_{\mathrm{vdW}}^{1-2} = -\frac{C_6}{d^6}, \tag{4}$$

where the strength of interaction is given by:

$$C_6 = \frac{3}{\pi}\int_0^\infty \alpha_1(\mathrm{i}u)\alpha_2(\mathrm{i}u)\mathrm{d}u. \tag{5}$$

Here $\alpha_j(\omega)$ is the polarizability at imaginary frequency $\omega = \mathrm{i}u$ of atom j, calculated from the dielectric response (3) using the expression

$$\alpha_j(\mathrm{i}u) = \frac{1}{E_0(\mathrm{i}u)}\int \mathrm{d}^3 r\, P(\mathbf{r}, \mathrm{i}u), \tag{6}$$

which relates $\alpha_j(\omega)$ with the polarization $P(\mathbf{r}, \omega)$ and the external field $E_0(\omega)$ (see [27] for details). Best results are obtained when the polarization

$$P = \chi E = \frac{\epsilon - 1}{4\pi}E \tag{7}$$

(and hence $\alpha_j(\mathrm{i}u)$) is determined self-consistently, taking into account that the total field $\mathbf{E}(\mathbf{r}, \mathrm{i}u)$ is the superposition of the constant external field $E_0(\mathrm{i}u)$ and the field induced by the polarization at other points [27].

In fact, the asymptotic atom–atom interaction, i.e. the value of C_6, is rather accurately known from other sources, such as empirical potentials and various many-body calculations [12], and the above calculation serves mainly as a testing ground for the present approach.

The atom–surface interaction is more subtle. Following the standard procedure explained in [29], in which the atom–surface vdW interaction is expressed in terms of the electronic response functions $\chi(\mathbf{r}, \mathbf{r}', \omega)$ of isolated fragments (and thereby also in terms of $\epsilon(\mathbf{r}, \omega)$ defined above), one arrives at the expression for the leading term in the asymptotic expansion of van der Waals interaction energy between an atom and a surface:

$$E_{\mathrm{vdW}}^{\mathrm{at-surf}} = -\frac{C_3}{(z - Z_0)^3}, \tag{8}$$

where C_3 is the strength of the interaction and Z_0 is the position of the effective van der Waals plane. The strength of the interaction is given by the Lifshitz-like expression:

$$C_3 = \frac{1}{4\pi}\int_0^\infty \alpha_{\mathrm{a}}(\mathrm{i}u)\frac{\epsilon_{\mathrm{b}}(\mathrm{i}u) - 1}{\epsilon_{\mathrm{b}}(\mathrm{i}u) + 1}\mathrm{d}u. \tag{9}$$

Here $\alpha_{\mathrm{a}}(\mathrm{i}u)$ is the atomic polarizability as explained above, and $\epsilon_{\mathrm{b}}(\mathrm{i}u) = \epsilon_{\mathrm{s}}(z, \mathrm{i}u)|_{z=-\infty}$ is the local dielectric function of the substrate far inside the bulk. The effective position of the vdW plane is obtained as [29, 30]:

$$Z_0 = \frac{1}{4\pi C_3}\int_0^\infty \alpha_{\mathrm{a}}(\mathrm{i}u)\frac{\epsilon_{\mathrm{b}}(\mathrm{i}u) - 1}{\epsilon_{\mathrm{b}}(\mathrm{i}u) + 1}\,\frac{\epsilon_{\mathrm{b}}(\mathrm{i}u)}{\epsilon_{\mathrm{b}}(\mathrm{i}u) + 1}\,d(\mathrm{i}u)\mathrm{d}u, \tag{10}$$

where $d(\mathrm{i}u)$ is the frequency dependent centroid of the surface charge induced by a uniform external electric field perpendicular to the surface [31]. In the present approximation this is given by

$$d(\mathrm{i}u) = -\frac{1}{\chi(-\infty, \mathrm{i}u)}\int z\frac{\mathrm{d}\chi(z, \mathrm{i}u)}{\mathrm{d}z}\mathrm{d}z, \tag{11}$$

where

$$\chi(z, \mathrm{i}u) = \frac{1}{4\pi}\frac{\epsilon_{\mathrm{s}}(z, \mathrm{i}u) - 1}{\epsilon_{\mathrm{b}}(\mathrm{i}u) + 1}\,\frac{2\epsilon_{\mathrm{b}}(\mathrm{i}u)}{\epsilon_{\mathrm{s}}(z, \mathrm{i}u)}\,\theta(d(0) - z). \tag{12}$$

Here a cut-off at $z = d(0)$ has been introduced, where $d(0)$ is the static centroid of the induced surface charge, in order to prevent the unphysical response of the low-density tails of the electronic density, as explained above.

Since equations (8)–(12) assume translational invariance parallel to the surface, the calculations are in practice performed after averaging the DFT densities over the x–y plane. The quantity $d(0)$ can be calculated numerically as the extrapolation to zero field of the charge induced by a static external electric field in the z direction, also averaged over the x–y plane. The accurate evaluation of Z_0 is the key to the quantitative success of the theory.

2.2. Seamless approach to van der Waals interactions

The approach in [32–34] is more elaborate. The energy is calculated using a new DFT functional, in which the exchange–correlation terms are different from the usual ones. The approach aims at providing a theory in which the van der Waals forces are incorporated in a 'seamless' fashion, and hence applicable also to systems which cannot be divided into almost independent fragments. In such a formulation the GGA terms for the exchange energy are retained, although the question about the best choice of the semilocal term is still open, as discussed below. The LDA term for the local correlation energy is also retained, while the semilocal correlation is replaced by a fully nonlocal expression:

$$E_{\mathrm{c}}^{\mathrm{nl}} = \tfrac{1}{2}\int \mathrm{d}^3r\,\mathrm{d}^3r' n(\mathbf{r})\phi(\mathbf{r}, \mathbf{r}')n(\mathbf{r}'), \tag{13}$$

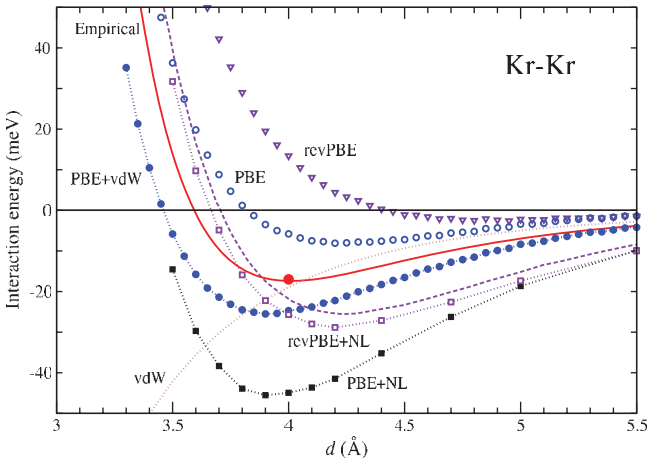

Figure 1. Comparison of different calculations of the interaction potential of a Kr dimer. Empty circles and triangles: DFT calculations for two flavours of GGA functional. Full circles and dotted line: GGA PBE calculation, with added vdW contribution. Full squares and dotted line: the calculation using the 'seamless' nonlocal expression for correlation, and PBE exchange. Empty squares and dotted line: same, but with revPBE exchange; a similar calculation from [34] is shown by dashed line, and the parameterized empirical potential from [35, 36] by a full line.

where the kernel $\phi(\mathbf{r}, \mathbf{r}')$ depends upon $(\mathbf{r} - \mathbf{r}')$ and the densities in the vicinity of $\mathbf{r}$ and $\mathbf{r}'$. The detailed form of the kernel is given in [34]. Qualitatively, the nonlocal functional is positive for small separations and becomes negative for larger separations. The positive contribution is analogous to the positive gradient terms in the GGA correlation, while the negative contribution at large separations gives rise to the vdW interaction. For a completely uniform electron density, E_c^{nl} vanishes and only the LDA correlation survives, as it should.

In order to compare the approach of [25–28] discussed in the preceding subsection with the nonasymptotic seamless approach of [32–34] on a fragmented system we have revisited the benchmark example of the Kr dimer studied earlier [34], for which accurate empirical and hybrid interaction potentials are available [35, 36]. In our calculations we have used the DACAPO program [37] with ultrasoft atomic pseudopotentials corresponding to the PW91 GGA functional and plane waves basis. In figure 1 we show the interaction energies of Kr_2 (i.e. the difference with respect to two separated atoms) at various interatomic distances d. The first two curves are calculated using the plain PBE and revPBE GGA functionals[3]. Also shown by a dotted line is the asymptotic vdW term $-C_6/d^6$ of the atom–atom interaction. Here the value of the coefficient C_6 was taken from [35] since our evaluation based on the DFT densities and the prescription of [25] gave the same result to within numerical uncertainties. We obtained the best agreement with reference results (empirical potential and the experimental value of the minimum shown by full line and heavy dot, respectively) using the sum of the PBE and vdW energies.

We have also performed calculations of the nonlocal expression for the correlation energy introduced in the seamless approach [34] (equation (13)), using the electronic density produced by the DACAPO program, for two choices of the exchange functional. The calculation with the PBE exchange shown in figure 1 yields the correct value of the equilibrium distance and

[3] Although the self-consistency is here achieved by using the PW91 GGA functional, the electron density is quite insensitive to this choice, as already discussed. The interaction energy calculated using PW91 and shown in [24] is clearly too large, and we shall not consider it here any more.

a good overall shape, but the interaction potential is too deep for more than a factor of two. The authors of [34] advocate the use of revPBE exchange, which is less attractive and does not produce spurious attractive interaction from the exchange alone, unlike some other GGA exchange functionals. We also show the results of our calculations with revPBE exchange, as well as those from [34] (dashed line) which differ by only a few millielectronvolts, obviously due to the details of the quite demanding numerical treatment of expression (13). While the depth of the attractive potential is in better agreement with the empirical potential and the experimental data than the results from the PBE exchange, the equilibrium distance is clearly too large and the whole repulsive part of the Kr–Kr potential energy appears too strong. In [38] the DFT with nonlocal correlation was applied to the more complex problem of binding energies of benzene dimers. The conclusions with regard to the choice of the GGA exchange are similar to ours, namely that the revPBE exchange energy is too repulsive at distances of interest, which leads to equilibrium distances which are too large. These authors then investigated the use of Hartree–Fock exchange energy instead, which gave results more like our calculations with PBE exchange, namely a binding energy which is too large but a position of the minimum which is in better agreement with the results derived from more complex *ab initio* calculations [38].

The above discussed results for the Kr dimer show that the approach of [25–28], in which the asymptotic vdW interaction between various fragments is added to the energies obtained in the usual DFT-GGA calculations, can be expected to provide good descriptions of the interactions involving noble gas atoms. The 'seamless' approach of [32–34] shows great potential, but, in addition to numerical complexity, the open question of the choice of the exchange part of the functional makes it at the moment less amenable to concrete applications.

3. Interfragment vdW interactions and structure of Xe adlayers

The problem of calculation of interactions that determine the structure of Xe adlayers on Cu(111) and Pt(111) surfaces reduces to a large extent to the question of a reliable representation of exchange and long-range correlation effects and thereby of vdW interactions by one of the approaches discussed in the previous section. The success of empirical binary potentials in describing some of the global properties of these systems [1] indicates that adsorbed Xe atoms can be considered as fragments fairly well separated from each other and from the atoms in the underlying substrate, among which only weak interactions are expected. However, despite the overall weakness of the interfragment Xe–Xe and Xe–substrate interactions their subtle character and mutual competition determine the adsorption site preference, equilibrium structure of adlayers, etc.

3.1. Self-supported Xe monolayers

Following the successful performance of the 'interfragment interaction' approach demonstrated in the preceding section on the paradigmatic example of Kr dimers, we adopt the same scheme for calculation of vdW interactions also in the Xe adlayer problem. We first evaluate the interaction energies of a self-supported (isolated) hexagonal Xe layer as a function of the nearest-neighbour distance d, using the DACAPO program. To check the transferability of the electronic density (i.e. the calculation of the electronic density using pseudopotentials and achieving self-consistency with a particular density functional, and then evaluating the energy with another one), we have repeated the calculations employing the ABINIT program [39] with norm-conserving native LDA and PBE-GGA pseudopotentials [40]. As shown in figure 2 the (non-self-consistent) DACAPO PBE and the (fully self-consistent) ABINIT PBE results agree

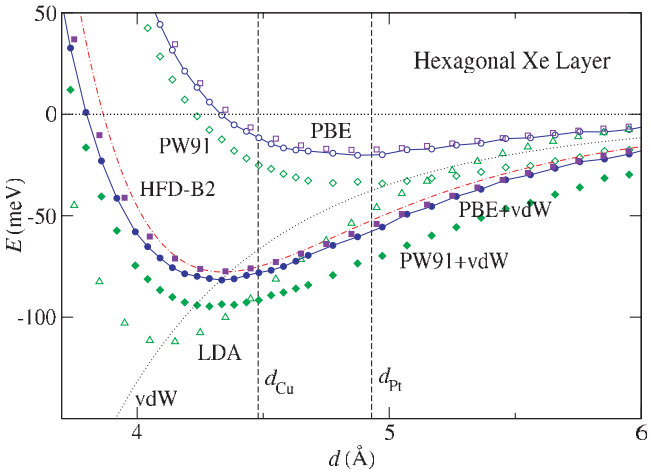

Figure 2. Total DFT-GGA interaction energy (per atom) of an isolated hexagonal layer of Xe atoms calculated as a function of nearest neighbour distance d without (open symbols) and with (full symbols) addition of the vdW component: PBE functional in ABINIT (○) and DACAPO (□), PW91 functional (◇), LDA without vdW only (△). Also shown is the the result obtained using the empirical HFD-B2 potential. Interatomic distances d_{Cu} and d_{Pt} corresponding to commensurate Xe layers on Cu(111) and Pt(111) surfaces are shown by vertical lines.

almost completely. Similar agreement is obtained for the LDA functional (not shown). We have also performed in-layer pairwise summation of the empirical HFD-B2 [12] binary Xe–Xe potential constructed to reproduce the Xe–Xe interactions in gas and condensed phases, and will henceforth consider the resulting sum as equivalent to an experimental quantity. We find that due to large interatomic distances the intralayer vdW interaction is not very sensitive to the model used and hence we evaluate it by summing the asymptotic pairwise contributions $-C_6/d_{ij}^6$ [25] and add it to DFT energies. In this approach the total interaction calculated from the empirical potential is again best reproduced by the combination of PBE and vdW potentials, with the minimum at $d_{min} = 4.3$ Å that nicely correlates with the interatomic distances measured at low temperatures in incommensurate ('floating') Xe monolayers on Cu(111) and Pt(111), and in bulk Xe [4, 41]. The interatomic distances $d_{Cu} = 4.48$ Å and $d_{Pt} = 4.80$ Å corresponding to commensurate adsorption on Cu(111) and Pt(111), respectively (see below), are also shown. The features of the results in figure 2 recur in all our calculations: the interaction energies calculated using GGA exhibit a shallow well with a minimum far out, but with inclusion of the vdW contribution the interaction agrees well with the empirical potential. On the other hand, the calculated LDA potential is largely overbinding even without the inclusion of the vdW attraction and is therefore clearly unphysical. Hence, the investigation of its applicability to the adsorption of Xe on Pt and Cu surfaces will not be pursued any further.

3.2. Commensurate Xe monolayers on Cu(111) and Pt(111)

In studies of Xe adsorption on Cu(111) and Pt(111) surfaces we follow the same rationale as discussed in the case of Kr dimers and a self-supported Xe monolayer. We employ the DACAPO DFT-GGA scheme complemented with the interfragment vdW interactions calculated by the approach developed in [25–28] and briefly reviewed in section 2.1. We first studied the adsorption of monolayer Xe on a Cu(111) surface. The substrate was modelled by six hexagonal atomic layers, of which the top three were allowed to relax. The undesired

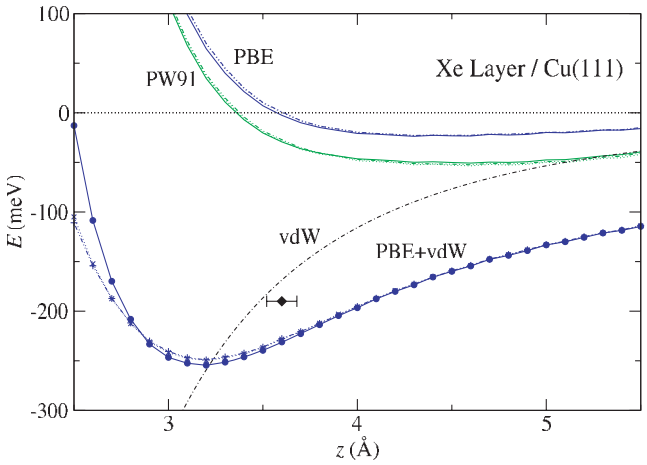

Figure 3. Total interaction energy (per adatom) of commensurate adlayer of Xe on a Cu(111) surface calculated using GGA functionals (see text), shown as a function of the distance z from the last substrate atomic plane. Upper sets, lines only: DFT-GGA results only, PW91 and PBE functionals. Lower set, lines and symbols: GGA-PBE functional with van der Waals contribution (dash–dot) added. ——•: Xe atoms in on-top sites, · · · · · ×: bridge sites, — · · —+: fcc hollow site. The diamond is the experimental value from [1, 6].

periodicity perpendicular to the surface was remedied by adding a thick vacuum slab above the Xe layer. The fcc lattice constant of the Cu substrate was 3.66 Å, namely equal to the equilibrium value obtained in our calculations for bulk Cu, which is about 1.4% larger than the experimental value of 3.61 Å. The supercell in x–y coordinates consisted of three Cu atoms in each substrate layer and one Xe atom in the overlayer, which corresponds to the experimentally observed $(\sqrt{3} \times \sqrt{3})$R30° structure. We have carried out calculations for the various separations z of the Xe layer from the outermost Cu(111) crystal plane. The asymptotic value of the calculated energy for large z is the 'desorption energy' of the entire Xe adlayer. To get the energy required to completely dissolve the Xe layer into isolated atoms, we subtracted the cohesive energy of the isolated Xe layer of the same geometry. Note that the experimental desorption energy may be smaller if measured at submonolayer Xe coverages for which the average cohesive energy per adatom is smaller.

Next we turn to the nonlocal interaction between the Xe layer and the substrate. The coefficient C_3 and the vdW reference plane position Z_0 in expression (8) for vdW interaction between an atom and the surface depend on the dynamic polarization of the substrate and the adatoms. We find the position of the static image plane $d(0)$ (see section 2.1) at 1.41 Å, outside the plane of the Cu nuclei in the first layer. The position Z_0 of the vdW plane calculated using the dynamic polarizability of Xe atoms is at 0.60 Å, i.e. shifted significantly closer to the position of Cu nuclei (cf figure 5 in [19]), which reflects the increased importance of the Cu d-orbitals in the high-frequency response of the substrate. We assume that the vdW interaction energies between the Xe atoms and the substrate are pairwise additive, as we did for the intralayer vdW interactions.

In figure 3 we show the results of DFT calculations for both the PW91 functional and the PBE functional, and the latter with the vdW contribution added. The PBE plus vdW result gives somewhat better agreement with experimental adsorption energies, but otherwise the two functionals differ only by an almost constant shift in energy. We have carried out the calculations for Xe atoms in on-top, bridge and hollow positions (fcc hollow and hcp

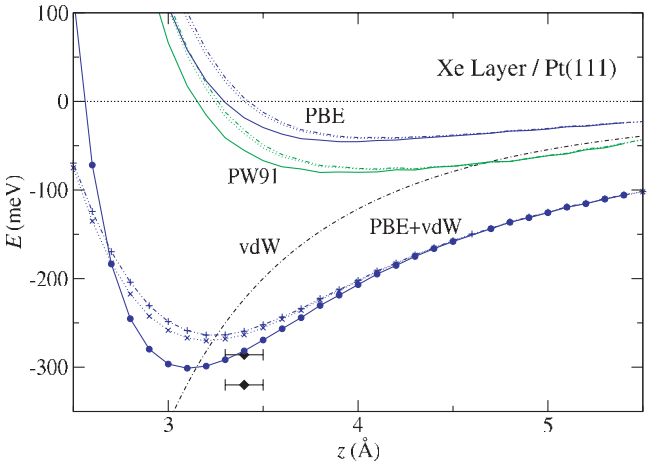

Figure 4. Similar as figure 3, but for Xe on a Pt(111) surface. Diamonds denote experimental results [8, 42].

hollow energies are virtually indistinguishable). The calculated DFT energy has a shallow minimum around 4.5 Å, where the bridge configuration has the lowest energy by a few millielectronvolts. However, at distances below 4 Å the energies for on-top site are lower due to the adsorption induced rearrangement of the substrate electronic density [18, 23]. Hence, when the interfragment vdW contribution is added (and also the intralayer energy at d_{Cu} from figure 2, which gives a constant offset), the on-top site is preferred by a few millielectronvolts, in accord with experiments. The adsorption distance $z_{\mathrm{min}} \simeq 3.20$ Å is in good agreement with the experimental value of 3.60 Å [6], and the PBE adsorption energy of 250 meV is somewhat larger than the reported experimental value of 190 meV [1]. The Xe adlayer on Cu(111) appears to be at the edge of instability of the incommensurate structure since the energy gain per atom of 3.1 meV, which would be achieved by reducing the Xe–Xe distance to the optimal value d_{min}, is similar to the energy loss incurred by the fact that some atoms should sit outside the on-top sites. The latter quantity is estimated from the energy of various configurations in figure 3 at z_{min}, where the differences between the on-top versus bridge and hollow site configurations are 2.1 and 3.8 meV, respectively. Indeed, experimental indications of a commensurate–incommensurate transition have been detected below 77 K [4].

Analogous calculations were performed for Xe on Pt(111), using the calculated Pt bulk lattice constant of 4.00 Å, while the experimental one is 3.92 Å. The results shown in figure 4 are qualitatively similar to the case of Cu(111). Here the preference for on-top sites is strongly reinforced by the vdW interaction, and the on-top PBE adsorption energy of 300 meV at $z_{\mathrm{min}} = 3.1$ Å is favoured by 34.5 meV compared to bridge sites and by 43 meV compared to hollow sites. The on-top commensurate Xe monolayer is nevertheless close to instability since the energy per atom due to the intralayer interaction is 23 meV higher at d_{Pt} than at d_{min} (cf figure 2).

4. Vibrational properties of Xe adlayers

In order to discuss the vibrational properties of commensurate Xe adlayers on Cu(111) and Pt(111) we have performed the analysis outlined in [9, 10, 14] by using our calculated potentials. Quite generally, adsorbed monolayers support three adlayer localized modes or

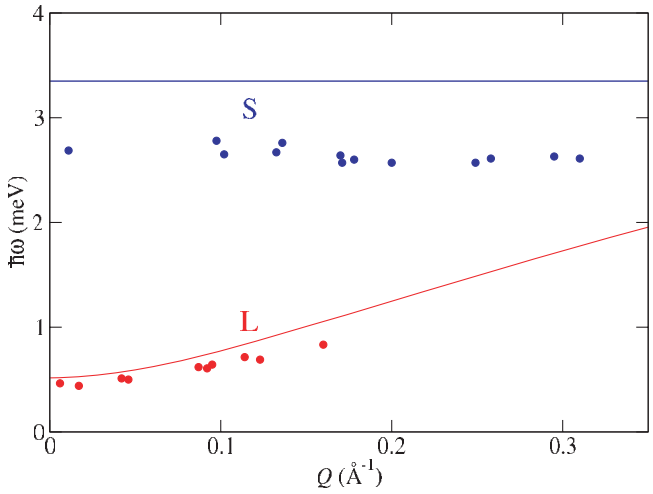

Figure 5. Theoretical Xe–adlayer L- and S-mode frequencies (lines) compared with experimental values (points) measured in HAS from Xe/Cu(111) in the $\bar{\Gamma}\bar{\mathrm{K}}$ direction of the adlayer [9].

phonons, characterized by the in-surface-plane wavevector **Q** and the polarization vector $\mathbf{e}_\kappa$. The latter is either dominantly perpendicular to **Q** and to the surface plane (vertically polarized mode κ = S), in-plane parallel to **Q** (longitudinally polarized mode κ = L) or in-plane perpendicular to **Q** (shear horizontally polarized mode κ = SH). Experimental S-mode frequencies measured by HAS for Xe/Cu(111) [9, 10] and Xe/Pt(111) [14] exhibit practically no dispersion for **Q** in the first surface Brillouin zone (SBZ) of the adlayer. Radial force constants β that determine these Einstein-like mode frequencies are calculated from the curvature around the on-top site minima of the potentials shown in figures 3 and 4. We find $\beta_{\mathrm{Xe-Cu}} = 5.7\ \mathrm{N\ m^{-1}}$ and $\beta_{\mathrm{Xe-Pt}} = 12.3\ \mathrm{N\ m^{-1}}$, yielding $\hbar\omega_{\mathrm{S}}^{\mathrm{Cu}} = 3.35$ meV (exp. 2.7 meV [9]) and $\hbar\omega_{\mathrm{S}}^{\mathrm{Pt}} = 4.93$ meV (exp. 3.7 meV [14]). Here the degree of agreement with experiment is the same (Cu) or better (Pt) than in earlier *ab initio* calculations [18, 22].

The tangential Xe–substrate force constants α which determine L- and SH-mode frequencies at the SBZ centre $\bar{\Gamma}$ ($Q = 0$) can be derived from the corrugation of Xe–Cu(111) and Xe–Pt(111) potential energy surfaces, assuming that the on-top site is the minimum and the bridge and hollow sites are the maxima of a two-dimensional cosine potential. For Cu, the energy of the on-top configuration is more favourable by 2.1, 3.7 and 3.8 meV compared to bridge, hcp hollow and fcc hollow configurations, respectively, while the lateral distance from the on-top site to bridge site is 1.29 Å and to fcc and hcp hollow sites is 1.48 Å. This gives (on average) $\alpha_{\mathrm{Xe-Cu}} = 0.134\ \mathrm{N\ m^{-1}}$. The energy differences for Xe/Pt are larger (cf figure 4), so that $\alpha_{\mathrm{Xe-Pt}} = 1.26\ \mathrm{N\ m^{-1}}$. The resulting $Q = 0$ limit of L- and SH-mode frequencies are $\hbar\omega_0^{\mathrm{Cu}} = 0.51$ meV and $\hbar\omega_0^{\mathrm{Pt}} = 1.58$ meV. The HAS data for the L-mode are ∼0.45 meV in Xe/Cu(111) [9], and 1.7 meV for Xe/Pt(111) (the last value extrapolated from $Q \simeq 0.2$ Å [14] that is the smallest Q for which the experimental data are available).

Dispersion of the L-mode (and also of the SH-mode, inaccessible in standard HAS measurements) for $Q > 0$ is dominantly determined by the intralayer radial force constants $\beta_{\mathrm{Xe-Xe}}$ [9, 10, 14]. We assume that the Xe–Xe interaction in *adsorption dilated* Xe adlayers is essentially the same as in an isolated Xe layer (figure 2). We use d_{Cu} and d_{Pt} corresponding to calculated bulk lattice constants of Cu and Pt, which are slightly larger (1.4% and 2%, respectively) than the experimental values. This leads to some additional uncertainty in

the values of the force constants calculated below, but since the deviations of d_{Cu} and d_{Pt} from the Xe–Xe potential minimum d_{min} are clearly larger, at 4% and 12%, respectively, the *qualitative* conclusion about the softening of force constants is not affected. Thus we find $\beta_{Xe-Xe}(d_{Cu}) = 0.76\ \mathrm{N\,m^{-1}}$, much lower than at d_{min} for an isolated Xe layer. For Pt we find $\beta_{Xe-Xe}(d_{Pt})$ to be virtually zero, which is not worrying as the corrugation of the Xe–substrate potential which pins the Xe lattice to the commensurate on-top structure prevents any instability. From this we find the dispersion of the L-mode in Xe/Cu(111) shown in figure 5 that is in excellent accord with the HAS data [9]. For in-plane modes in Xe/Pt(111) we find practically no dispersion, $\hbar\omega^{Pt}(\mathbf{Q}) \simeq \hbar\omega_0^{Pt}$, also in accord with experiment [14].

5. Conclusions

In this paper we have demonstrated the necessity of including the van der Waals interactions in the DFT-based calculations of the potential energy surfaces describing prototype weak adsorption systems of Xe/metal surfaces. By testing and analysing the performance of the currently used DFT approaches that incorporate the van der Waals interactions in the calculations of total energies of weakly bound systems, we have found that for a paradigmatic example of a Kr dimer the DFT-GGA approach complemented with a DFT-derived interfragment treatment of vdW forces yields the best agreement with the results of experiments and the various empirical and hybrid approaches available for this system. By extending the same treatment to the calculations of ground state energies, structural and vibrational properties of Xe monolayers on Cu(111) and Pt(111) surfaces, we have obtained *ab initio* results that are so far in very close agreement with experiment. This affirms the potential of such generalized first principles approach for studying the properties of a wide class of weakly bound fragmented systems. In addition, our exhaustive studies of the reliability of the various DFT approximations in combination with the interfragment approach also pinpoint its limitations that could be remedied in the recently proposed seamless approaches [32–34, 43] aimed at providing a unified treatment of dynamic polarization interactions at all interatomic separations.

Acknowledgment

This work was supported by the Ministry of Science and Technology of the Republic of Croatia under contract nos 098-0352828-2863 and 035-0352828-2839.

References

[1] Bruch L W, Cole M W and Zaremba E 1997 *Physical Adsorption: Forces and Phenomena* (Oxford: Claredon)
[2] Vidali G, Ihm G, Kim H-Y and Cole M W 1991 *Surf. Sci. Rep.* **12** 133
[3] Steele W A 1973 *Surf. Sci.* **36** 317
[4] Jupille J, Erhardt J-J, Fargues D and Cassuto A 1990 *Faraday Discuss. Chem. Soc.* **89** 323
Jupille J, Erhardt J-J, Fargues D and Cassuto A 1990 *Vacuum* **41** 399
[5] Kern K, David R, Palmer R L and Comsa G 1986 *Phys. Rev. Lett.* **56** 620
[6] Seyller Th, Caragiu M, Diehl R D, Kaukasoina P and Lindroos M 1998 *Chem. Phys. Lett.* **291** 567
[7] Gottlieb J M 1990 *Phys. Rev.* B **42** 5377
[8] Seyller Th, Caragiu M, Diehl R D, Kaukasoina P and Lindroos M 1999 *Phys. Rev.* B **60** 11084
[9] Braun J, Fuhrmann D, Šiber A, Gumhalter B and Wöll Ch 1998 *Phys. Rev. Lett.* **80** 125
[10] Šiber A, Gumhalter B, Braun J, Graham A P, Bertino M F, Toennies J P, Fuhrmann D and Wöll Ch 1999 *Phys. Rev.* B **59** 5898
[11] Gumhalter B 2001 *Phys. Rep.* **351** 1

[12] Dham A K, Meath W J, Allnatt A R, Aziz R A and Slaman M J 1990 *Chem. Phys.* **142** 173
Kumar A and Meath W J 1985 *Mol. Phys.* **54** 823
[13] Boas Ch, Kunat M, Burghaus U, Gumhalter B and Wöll Ch 2003 *Phys. Rev.* B **68** 075403
[14] Bruch L W, Graham A P and Toennies J P 1999 *Mol. Phys.* **95** 579
[15] For a review of DFT applications to atom–surface interactions see Brivio G P and Trioni M I 1999 *Rev. Mod. Phys.* **71** 231
[16] Lang N D 1981 *Phys. Rev. Lett.* **46** 842
[17] Müller J E 1990 *Phys. Rev. Lett.* **65** 3021
[18] Bagus P S, Staemmler V and Wöll Ch 2002 *Phys. Rev. Lett.* **89** 096104
[19] Wandelt K and Gumhalter B 1984 *Surf. Sci.* **140** 355
[20] Hotzel A, Moos G, Ishioka K, Wolf M and Ertl G 1999 *Appl. Phys.* B **68** 615
[21] Pérez R, García-Vidal F J, de Andrés P L and Flores F 1994 *Surf. Sci.* **307–309** 704
[22] Betancourt A E and Bird D M 2000 *J. Phys.: Condens. Matter* **12** 7077
[23] Da Silva J L F, Stampfl C and Scheffler M 2003 *Phys. Rev. Lett.* **90** 066104
Da Silva J L F, Stampfl C and Scheffler M 2005 *Phys. Rev.* B **72** 075424
[24] Lazić P, Crljen Ž, Brako R and Gumhalter B 2005 *Phys. Rev.* B **72** 245407
[25] Andersson Y, Langreth D C and Lundqvist B I 1996 *Phys. Rev. Lett.* **76** 102
[26] Hult E, Andersson Y and Lundqvist B I 1996 *Phys. Rev. Lett.* **77** 2029
[27] Hult E, Rydberg H, Lundqvist B I and Langreth D C 1999 *Phys. Rev.* B **59** 4708
[28] Hult E, Hyldgaard P, Rossmeisl J and Lundqvist B I 2001 *Phys. Rev.* B **64** 195414
[29] Zaremba E and Kohn W 1976 *Phys. Rev.* B **13** 2270
[30] Persson B N J and Zaremba E 1984 *Phys. Rev.* B **30** 5669
[31] Feibelman P J 1982 *Prog. Surf. Sci.* **12** 287
[32] Rydberg H, Dion M, Jacobson N, Schröder E, Hyldgaard P, Simak S I, Langreth D C and Lundqvist B I 2003 *Phys. Rev. Lett.* **91** 126402
[33] Langreth D C, Dion M, Rydberg H, Schröder E, Hyldgaard P and Lundqvist B I 2005 *Int. J. Quantum Chem.* **101** 599
[34] Dion M, Rydberg H, Schröder E, Langreth D C and Lundqvist B I 2004 *Phys. Rev. Lett.* **92** 246401
[35] Tang K T and Toennies J P 2003 *J. Chem. Phys.* **118** 4976
[36] Wu X, Vargas M C, Nayak S, Lotrich V and Scoles G 2001 *J. Chem. Phys.* **115** 8748 and references therein
Scoles G 2006 private communication
[37] http://www.fysik.dtu.dk/campos/Dacapo
[38] Puzder A, Dion M and Langreth D C 2006 *J. Chem. Phys.* **124** 164105
[39] Gonze X *et al* 2002 *Comput. Mater. Sci.* **25** 478
[40] Fuchs M and Scheffler M 1999 *Comput. Phys. Commun.* **119** 67
[41] Bruch L W, Graham A P and Toennies J P 2000 *J. Chem. Phys.* **112** 3314
[42] Widdra W, Trischberger P, Frieß W, Menzel D, Payne S H and Kreuzer H J 1998 *Phys. Rev.* B **57** 4111
[43] Kohn W, Meir Y and Makarov D E 1998 *Phys. Rev. Lett.* **80** 4153